Parametric study of tire pavement contact under dynamic traffic loads

Aziza El Ghoulbzouri [1] and Abdelouafi El Ghoulbzouri [1]

[1]Abdelmalek Essaadi University, Tétouan, MOROCCO.elghoulbzouri.aziza@etu.uae.ac.ma

Abstract. This work centers on the development of a three-dimensional tire–pavement interaction model in order to study the distribution of contact stresses, for future use in mechanistic analysis of pavement behavior. Using the finite element method within the Abaqus code, a longitudinal tread tire and an elastic asphalt pavement were modeled. The contact area and stress distribution were simulated under steady-state, rolling, and braking conditions, incorporating dynamic traffic loads. Pavement roughness was analyzed by considering different friction coefficients, and a parametric study was conducted on tire inflation pressure and rolling speed. Moreover, the study examined the effect of pavement geometry by considering different road camber and rut depth. The findings indicate that both inflation pressure and tire friction coefficient significantly influence the 3D contact stress distribution as well as the road camber and rut depth.

Keywords: Tire-pavement contact, finite element method, dynamic responses, rolling, braking.

1 Introduction

The asphalt pavement deterioration is mainly caused by pavement vehicle interactions, [8]. To have an accurate design and analysis, it is crucial to study the asphalt pavement behavior under dynamic loads. Based on the elastic layer theory, the mechanical-empirical road design technique treats the pavement structure as an elastic structure. Due to its computation simplicity, this assumption which assumes that the traffic load is concentrated or distributed linearly over the entire width of the wheel has been widely used, [6]. Moreover, particularly in Morocco, the dimensioning of the pavement layers is based on catalogs. these catalogs remain limited in information and require periodic updates. Nevertheless, the tire pavement interaction and material properties plays a crucial role in asphalt pavement mechanical response.

Even though analytical solutions are efficient in calculating pavement response, their scope of usage and the accuracy results are limited because of many simplifying as-

sumptions use. Additionally, analytical solutions are typically not adaptable to advanced problems, [12]. Due to its ease of use and high efficiency compared to the analytical method, numerical methods such as the finite element method (FEM) have gained popularity for pavement mechanical analysis.

The tire pavement interaction implies a complex stress distribution that increases significantly the risk of degradations such as rutting and cracking. Current design methods of asphalt pavement tend to simplify this interaction by presuming a circular tire-pavement contact zone and a uniformly distributed vehicle load which is an idealization that does not accurately reflect actual field conditions [5]. As a result, in finite element analysis, it becomes challenging to seek accurate prediction of pavement damage, induced by heavy vehicles, tends to initiate at the surface when using uniform loads [5, 9]. To overcome this limitation, it is crucial to investigate the detailed tire–pavement contact and the associated stress complexities so as to better understand the dynamic response of pavement structures.

Tire–pavement contact stress is a multidimensional phenomenon composed of three components: vertical, longitudinal, and transverse stresses, each one contributes uniquely to the load transfer mechanisms acting on the pavement surface [9, 11]. Unlike the simplified assumption of a uniform pressure distribution, real-world contact stresses are Significantly irregular and present an important spatial variability. This complexity results from the interplay of many influencing factors. Among the most critical, we find the type and construction of the tire, which determine the contact area geometry and stiffness characteristics; the inflation pressure, which impacts the size and shape of the contact patch; and the magnitude of the applied load, which modifies the stress intensity and distribution [4, 10, 11].

Moreover, dynamic rolling conditions and the tilting or camber angle of the tire [7] introduce additional asymmetry in stress patterns. The pavement surface texture also plays a crucial role [3], generate localized stress concentrations that can accelerate the early onset of damage. Together, these factors create a highly complex and non-uniform stress field at the tire–pavement contact zone, making accurate modeling critical for realistic analysis of pavement response and long-term performance.

This paper's main goal is to create a 3D tire-pavement simulation using the finite element method. The 3D contact stresses distribution under steady state, rolling, and braking conditions were simulated and analyzed.

The objective required the following actions:

- Considering the parameters of tire manufacturers, a 3D model of a tire is developed based on geometric structure and tire size.
- Developing a three-dimensional interaction simulation between the tire and pavement.
- Using the model to predict contact stresses of tire-pavement interface for multiple inflation pressures, friction coefficients, asphalt pavement geometries, and different rolling velocities during different rolling conditions.

2 Model Description

The simulation model of the dynamic friction due to tire-pavement contact was created to perform three rolling regimes: steady state (force was applied for a sufficient time to stabilize the vibrations), rolling (rapid acceleration then constant speed), and braking. Concerning the boundary conditions (BCs), symmetry conditions were applied to the five non-free surfaces of the pavement. Tire rolling includes the angular velocity ω and linear velocity V. Additional BCs were applied to the reference point RP1 (master point attached to the center of the tire via a kinematic coupling) to avoid any undesired movement and/or rotation of the tire. To minimize the vibrations due to the dynamic movement and numerical effect (due to the explicit resolution of the equation system), a spring/damper system was used linking the two reference points RP1 (attached to the center of the tire) and RP2 (attached to the unmodeled vehicle). The simulated tire load was F=30 kN. The considered tire characteristics were 315/80R22,5. **Fig. 1** shows the dimensions and features of the model as well as the tire cross-section profile.

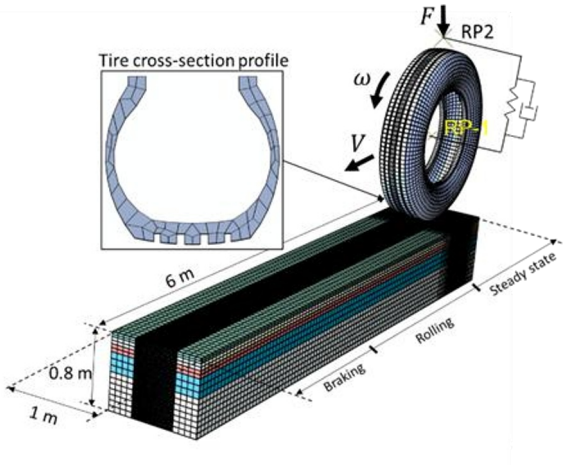

Fig. 1. FE tire-pavement model

The pavement was considered elastically deformable (**Table 1** outlines the pavement structure and material parameters) and the tire was hyperelastic. The Neo-Hookean model was selected to describe the constitutive relationship of hyperelasticity (see **Table 2**). The friction coefficient μ (at the tire-pavement interface) is modelled with the modified Coulomb model considering the slip stress limitation, written as follows:

$$\tau_f = \min\left(\bar{\tau}, \mu\sigma_n\right) \tag{1}$$

where $\bar{\tau}$ is the current shear flow stress of the material at the contact interface, and σ_n the normal stress.
The static friction coefficient (Equation (2)) is defined in the initial contact phase (the tire is about to slide), in which the tire velocity is zero.

$$\mu = T / N \tag{2}$$

where T is the tangential force between tire and pavement contact and N is the normal force (perpendicular to the contact surface).

Table 1. Pavement material properties, [1]

Layer material	Thickness (mm)	Elastic Modulus (MPa)	Poisson's Ratio	Density (Kg/m^3)
EB	50	36000	0.35	2340
GBB	70	7000	0.35	2320
GBB2	80	5000	0.35	2320
GNF1	200	400	0.35	2200
Infini	400	20	0.35	2200

Table 2. Tire material properties, [2]

Neo-Hookean model parameters		Density (Kg/m3)
C10 (MPa)	D1 (MPa)	
1.803	0	1184

3 Parametric Study

Before carrying out the parametric studies, a first study was performed to analyze the effect of the mesh on the results. For this, three pavement meshes were simulated: coarse, medium, and refined mesh. The mesh was modified only in the contact area. The tire mesh was kept the same for the three simulations. The inflation pressure P=0.85 MPa, and μ=0.7 and the longitudinal velocity of the tire V=60km/h were chosen for this first study.

Five parameters were studied in this paper, the inflation pressure P, friction coefficient μ, rolling speed V, road camber α and the rut depth D. **Table 3** shows the values chosen. **Fig. 2** shows the shape of the studied road camber and rut depths.

Table 3. Values of the studied parameters.

P (MPa)	μ	V (km/h)	α (°)	D (mm)
0.5	0.2	60	2.5	6
0.6	0.35	80	4	13
0.7	0.54	100	7	25
0.85	0.7			

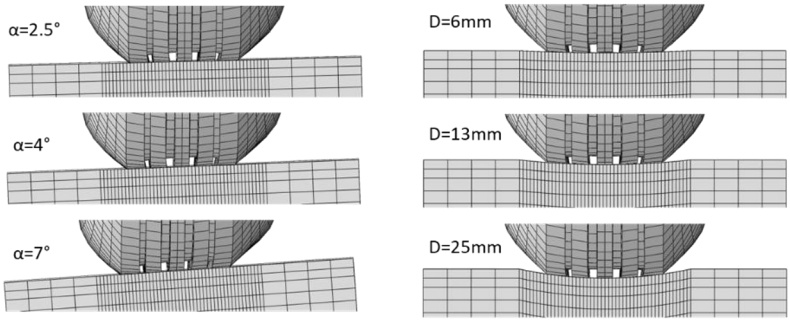

Fig. 2. Road camber and rut depth studied

4 Analyses And Results

Mesh refinement is important particularly when the explicit method is used to solve a contact problem. In fact, according to the results of **Fig. 3** (representing the imprint of the tire on the pavement surface during the rolling regime), it can be seen that the smaller the mesh size, the better the representation of the tire-pavement contact. With a refined mesh (**Fig. 3** (c)), the presence of the grooves in the tire is noticeable contrary to the coarse mesh cases.

However, contrary to an implicit resolution, the explicit method strongly depends on the mesh size considerably impacting the CPU calculation time. Indeed, the CPU time is 5 times greater with a refined mesh than with a coarse one (please see **Table 4**). For this reason, the following simulations were carried out with the medium mesh to be reasonable both on the results accuracy and the calculation times.

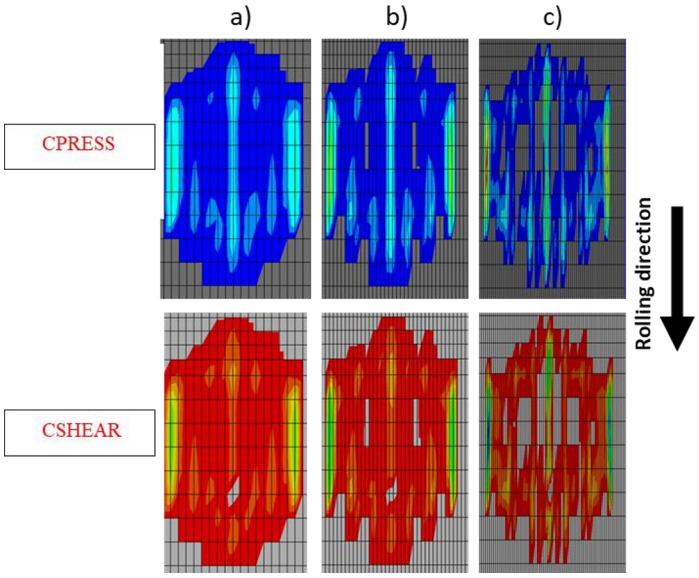

Fig. 3. Pressure (CPRESS) and shear stress (CSHEAR) for a) coarse, b) medium, and c) refined mesh.

Table 4. Mesh size and calculation time.

Mesh size	**Refine**	**Medium**	**Coarse**
Number of elements	156115	87072	53285
Calculation time (h)	10	3	2

Fig. 4 shows the results of the simulations for a friction coefficient μ=0.54 during the three traffic regimes (steady state, rolling, and braking). In this figure, the contact pressure along the path in the middle of the imprint (see **Fig. 4** (a)) was plotted for different values of inflation pressure. Overall observation, the pressure is maximum at the extremities whatever the inflation pressure for both steady state and braking regimes. However, it is rather localized in the middle with a considerable reduction in its width during the rolling regime.

In the case of steady-state and braking, the contact pressure decreases with the increase of inflation pressure, particularly at the extremities. It can be observed that the contact pressure tends to be equal between the middle and extremities. Since the reinforcement of the tire was not considered in the simulations, the middle of the tire remains sensitive to deflection. However, in **Fig. 4** (c) the contact pressure increases with the inflation pressure.

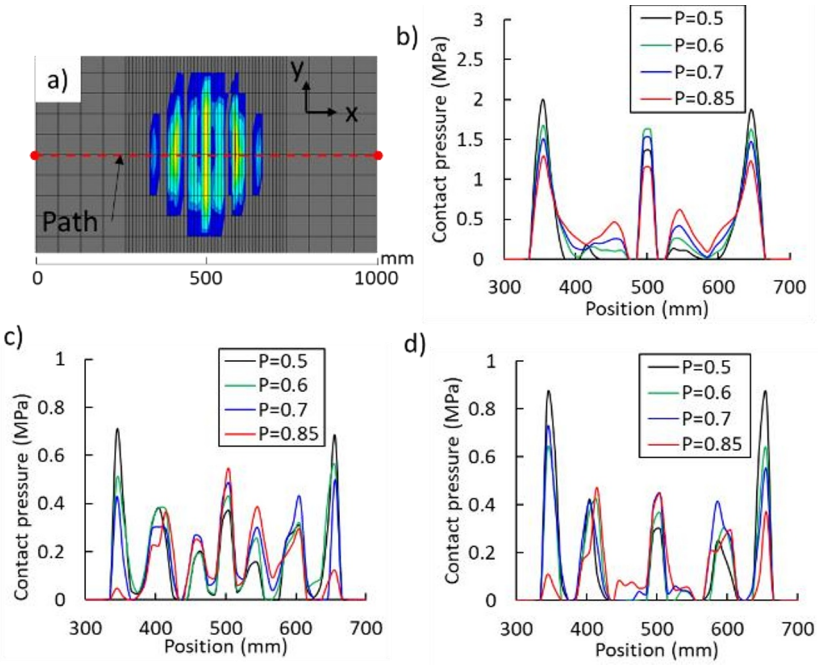

Fig. 4. Contact stresses for μ=0.54 and different inflation pressure during: b) steady state, c) rolling, and d) braking.

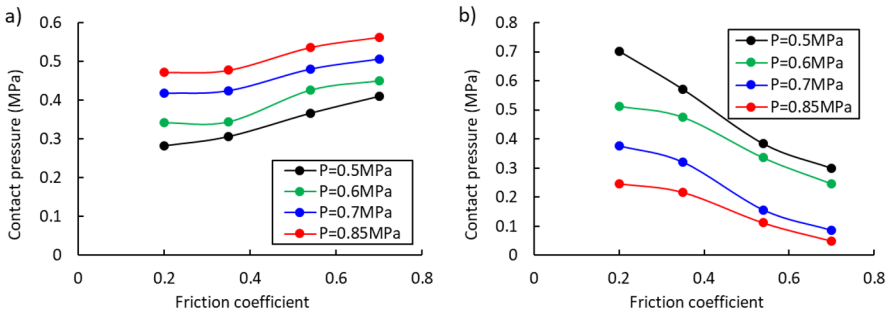

Fig. 5. Contact stresses in a) the middle (at x=500 mm), and b) the extremity (at x=344 mm) of the surface contact during the rolling regime.

Fig. 5 shows the variation of the contact pressure during the rolling regime as a function of the friction coefficient for different inflation pressure values in middle (at x=500 mm), and the extremity (at x=344 mm) of the surface contact. A high inflation pressure reduces the contact area, concentrating pressure in the middle of the tire footprint and decreasing it at the extremities, whereas a lower pressure promotes a more even distribution, and increases pressure at the extremities when the inflation pressure is very low. The friction coefficient also influences this distribution: on a rigid pavement, contact pressure is more uniform between the middle and the extremities, while on a flexible pavement, it is more concentrated in areas where the tire sinks, often at the middle if the inflation pressure is high. Thus, a high inflation pressure combined with a flexible pavement increases pressure concentration in the middle, whereas a lower pressure and a rigid pavement promote a more balanced distribution between the middle and the extremities.

The friction coefficient effect has a more pronounced impact on the shear stress than on the normal pressure. **Fig. 6** (a) and **Fig. 6** (b) show the variation of the shear stress during the braking regime as a function of the friction coefficient for different inflation pressure values in middle (at x=500 mm), and the extremity (at x=344 mm) of the surface contact respectively. When the vehicle brakes, the distribution of shear stress varies depending on tire pressure and contact position. In the middle, high pressure reduces the contact area, concentrating shear stress, while low pressure expands it, distributing the force more evenly. At the extremities, high pressure limits contact and decreases stress, whereas low pressure increases adhesion and load on these areas.

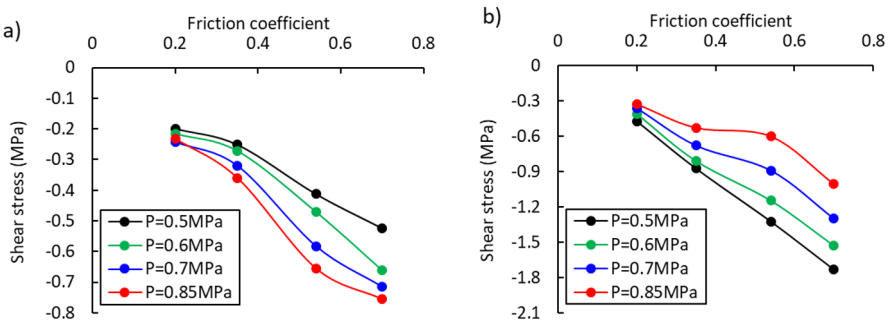

Fig. 6. Shear stresses in a) the middle (at x=500 mm), and b) the extremity (at x=344 mm) of the surface contact during the braking regime.

Fig. 7 shows the results of the simulations for a friction coefficient μ=0.54 during the three traffic regimes (steady state, rolling, and braking). When the wheel spins at high speed, centrifugal forces appear and affect the shape of the tire. Due to these forces, the particles in the tread tend to move away from the center of rotation, causing an increase in the tire's radius and making it slightly larger at high speeds. This expansion reduces the contact pressure at the center of the footprint on the ground and may shift part of the contact toward the edges of the tire. Additionally, at low speed, the tire deforms more upon contact with the ground, as the carcass has time to flex and adapt to the surface. However, at high speed, centrifugal force slightly stiffens the tread, reducing flexion and altering the shape of the contact area. As a result, the contact pressure may become more uniform or shift slightly toward the outer part of the tire.

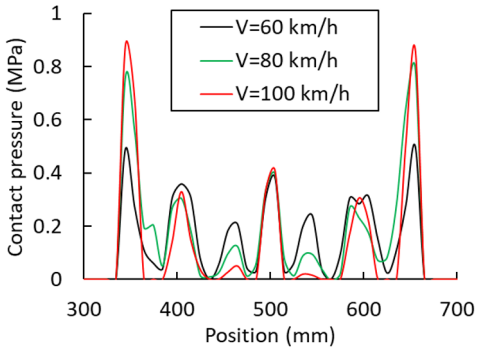

Fig. 7. Contact stresses for μ=0.54 and different velocities during rolling.

During the rolling regime, the contact pressure gradually develops an asymmetric distribution: it increases at one extremity of the contact imprint and decreases et the opposite extremity, potentially dropping to zero when the camber angle becomes significantly high (e.g., α=7°). The same conclusions are obtained for the shear stresses during braking regime (see **Fig. 8**).

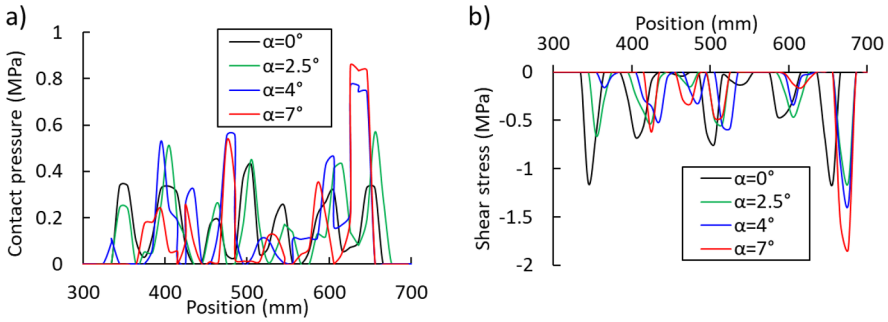

Fig. 8. a) Contact stresses during rolling and b) Shear stresses during breaking for μ=0.54, P=0.6MPa and different road camber.

In **Fig. 9**, the rut depth has an important influence on the stress distribution at the edges of the patch. These regions are subjected to intensified loading during both rolling and braking regimes, which make them more vulnerable to damage. Meanwhile, the middle of the contact area is experiencing relatively lower stress variation. This non-uniform loading pattern contributes to the early crack's initiation of rutted paths, highlighting a critical area for pavement deterioration and structural failure.

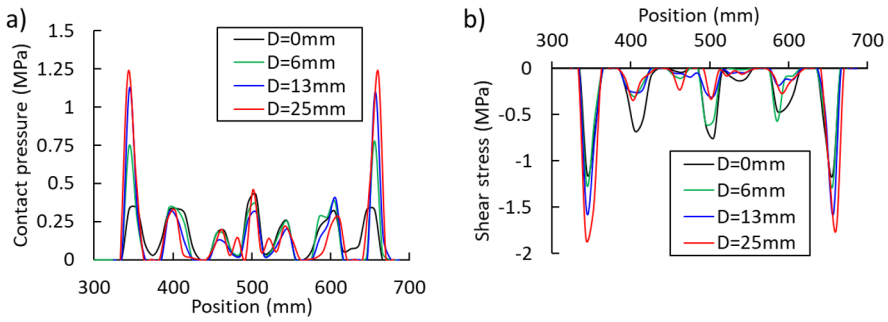

Fig. 9. a) Contact stresses during rolling and b) Shear stresses during breaking for μ=0.54, P=0.6MPa and different rut depth.

5 Conclusion

To analyze contact stresses under steady state, rolling, and braking conditions, the tire-pavement contact model was developed using the FEM. A parametrical study was performed to better understand the effect of several parameters.
The results indicate that:

- In steady state and braking conditions, the contact pressure is more important at the extremities.
- Rolling condition is characterized by the important contact pressure in the middle as the inflation pressure increases.

- During the braking regime, the friction coefficient affects considerably the shear stresses whatever the inflation pressure magnitude.
- At high speed, centrifugal forces cause the tire to expand slightly, increasing its radius and shifting contact pressure toward the extremities. This also stiffens the tread, reducing flexion and altering the contact area, making pressure more uniform or slightly displaced outward.
- The rut depth significantly affects stress distribution, causing higher stress and damage risk at the patch extremities, while road camber increases stresses in in the steeply inclined extremity.

Based on the results of this article, pavement design, and damage analysis for three-dimensional contact stress distribution between tire and pavement will be carried out in further work.

References

1. AFECHKAR M (2019) Dimensionnement des chaussées méthode Alizé, Ministère de l'équipement, du transport, de la logistique et de l'eau
2. Conradie JM, Els PS, Heyns PS (2016) Finite element modelling of off-road tyres for radial tyre model parameterization. Proc Inst Mech Eng Part J Automob Eng 230:564–578
3. Dong S, Han S, Luo Y, Han X, Xu O (2021) Evaluation of tire-pavement noise based on three-dimensional pavement texture characteristics. Constr Build Mater 306:124935
4. Gong Z, Miao Y, Lantieri C (2024) Review of research on tire–pavement contact behavior. Coatings 14:157
5. Jiang X, Zeng C, Gao X, Liu Z, Qiu Y (2019) 3D FEM analysis of flexible base asphalt pavement structure under non-uniform tyre contact pressure. Int J Pavement Eng 20:999–1011
6. Király T, Primusz P, Tóth C (2022) Simulation of static tyre–pavement interaction using two FE models of different complexity. Appl Sci 12:2388
7. Lee SI, Mwanza AD, Mutembo G, Walubita LF (2014) Effects of Tire Inclination on the HMA Pavement Shear Stress-Strain Response: 2-D Computational Modeling. In: Design, Analysis, and Asphalt Material Characterization for Road and Airfield Pavements. pp 41–48
8. Ma X, Dong Z, Dong Y (2023) Stiffness identification method for asphalt pavement layers and interfaces using monitoring data from built-in sensors. Struct Health Monit 22:151–165
9. Oubahdou Y, Wallace ER, Reynaud P, Picoux B, Dopeux J, Petit C, Nélias D (2021) Effect of the tire–pavement contact at the surface layer when the tire is tilted in bend. Constr Build Mater 305:124765
10. Wang C, Zhang J, Zhou H (2022) Analysis of Tire-Pavement Contact Morphology Characteristics during the Virtual Track Train Maneuvering. Adv Civ Eng 2022:1285552
11. Wang T, Dong Z, Xu K, Ullah S, Wang D, Li Y (2022) Numerical simulation of mechanical response analysis of asphalt pavement under dynamic loads with non-uniform tire-pavement contact stresses. Constr Build Mater 361:129711

12. Wu C, Wang H, Zhao J, Jiang X, Yanjun Q, Yusupov B (2020) Prediction of Viscoelastic Pavement Responses under Moving Load and Nonuniform Tire Contact Stresses Using 2.5-D Finite Element Method. Math Probl Eng 2020:1029089